

## Physical characteristics of $\text{LaCr}_x\text{Al}_{1-x}\text{O}_3$ : DFT approach

H. Javid<sup>a</sup>, S. A. Aldaghfag<sup>b</sup>, M. K. Butt<sup>a</sup>, S. Mubashir<sup>a</sup>, M. Yaseen<sup>a,\*</sup>, M. Ishfaq<sup>a</sup>, S. Saleem<sup>a</sup>, H. Elhosiny Ali<sup>c,d</sup>, H. H. Hegazy<sup>c,d</sup>

<sup>a</sup>*Spin-Optoelectronics and Ferro-Thermoelectric (SOFT) Materials and Devices Laboratory, Department of Physics, University of Agriculture Faisalabad 38040, Pakistan*

<sup>b</sup>*Department of Physics, College of Sciences, Princess Nourah bint Abdulrahman University, P. O. Box 84428, Riyadh 11671, Saudi Arabia*

<sup>c</sup>*Research Center for Advanced Materials Science (RCAMS), King Khalid University, Abha 61413, P. O. Box 9004, Saudi Arabia.*

<sup>d</sup>*Department of Physics, Faculty of Science, King Khalid University, P.O. Box 9004, Abha, Saudi Arabia.*

The magnetic, electronic, and optical properties of Cr doped  $\text{LaAlO}_3$  are examined by Full Potential linearized augmented plane wave (FP-LAPW) method within Density functional theory (DFT). The pure compound ( $\text{LaAlO}_3$ ) is doped with different concentrations of chromium (Cr) to examine the doping effects on its characteristics. The calculations of band structure (BS) and density of states show Cr has major contribution while La, Al and O atoms have little involvement in the states near Fermi level. The magnetic features revealed that Cr plays major participation in ferromagnetic nature of  $\text{LaCr}_x\text{Al}_{1-x}\text{O}_3$ . The results of electronic and optical revealed that the compound under study is suitable for spintronics and optoelectronics applications.

(Received March 28, 2022; Accepted July 1, 2022)

*Keywords:* DFT, Spintronics, doping, Perovskite materials

### 1. Introduction

Perovskite oxides have obtained significant attraction of scientist around the globe because of their unique characteristics like ferromagnetism, superconductivity, multiferroicity and colossal magnetoresistance [1-4]. All these properties make these materials exclusive for industrial and technological uses including memory devices, optoelectronics, solar cells, and transducers [5-7]. In recent years, diluted magnetic semiconductors have obtained much consideration due to their applications in spintronics devices [8,9]. Moreover, induction of ferromagnetism in nonmagnetic Perovskites compound is significant from experimentally and theoretically prospective because of spin functionality addition to host crystal [10-13]. In addition to this, multiferroic compounds are being obtained by doping of transition metal (TM)[14]. The TM ions exhibit intrinsic functionalities such as superconductivity, ferroelectricity, thermoelectricity, and magnetism [15,16].

Lanthanum Aluminate is most promising candidate in the family of perovskite oxides from theoretical and experimental point of view [17]. This compound has high value of dielectric permittivity, which is beneficial for different application like ferroelectric thin film microwave devices, high frequency capacitor and dielectric resonators [18]. When we introduce doping in intrinsic  $\text{LaAlO}_3$ , it has been found that the compound become suitable for manufacturing of eye safe laser as well as optical communication devices [19,20]. Moreover, the chromium doped  $\text{LaAlO}_3$  formulated by solid state reaction have shown suitability for vivo imaging applications [21]. Benam et al. investigated pressure effect on optical features of  $\text{LaAlO}_3$  by first principle which stated that the value of band gap ( $E_g$ ) increasing by increasing compression on system [22].

---

\* Corresponding author: myaseen\_taha@yahoo.com

<https://doi.org/10.15251/JOR.2022.184.481>

Boudali et al. observed the elastic, electronic, thermal as well as structural features of  $\text{LaAlO}_3$  and declared that this material is appropriate for optoelectronic applications [23].

In present work, the optical, magnetic, and electronic features of Cr doped  $\text{LaAlO}_3$  compounds have been analyzed by DFT. In electronic properties, BS, DOS and PDOS are calculated to observe the nature of material along with participation of elements. In optical properties, different parameters such as optical conductivity ( $\sigma(\omega)$ ), reflectivity ( $R(\omega)$ ), absorption coefficient ( $\alpha(\omega)$ ), dielectric constant, extinction coefficient ( $k(\omega)$ ) and refractive index ( $n(\omega)$ ) are computed. The magnetic properties are also examined to check the magnetic behavior of the material. There is no previous theoretical work on magnetic, optical, and electronic calculations of Cr doped  $\text{LaAlO}_3$  that encourages us to analyze its properties. Our calculated outcomes are beneficial to implement this compound for spintronics and optoelectronic applications.

## 2. Method of calculation

The FP-LAPW method within DFT applied in Wien2k code is utilized to examine the optical and electronic behavior of Cr doped  $\text{LaAlO}_3$  [24,25]. The wave function, charge density and potential are extended on two bases in FP-LAPW method. It can be observed that potential and wave function are expanded on spherical harmonic basis inside atomic sphere whereas plane waves are extended outside the atomic sphere. The potential in both areas can be explained by following relation:

$$V(r) = \begin{cases} \sum_{LM} V_{LM}(r) Y_{LM}(\hat{r}) & \text{inside sphere} \\ \sum_K V_K e^{iK \cdot r} & \text{outside sphere} \end{cases} \quad (1)$$

All constraints are precisely determined in the Hamiltonian of multiple body system by eliminating conversion association potential [26, 27]. The value of  $l_{max}$  is constant outside the sphere, whereas its value is taken as 10 inside the sphere. The 33 k-point sampling is utilized to make 1000 Monkrostr pack meshes grid. Moreover, RMT (muffin tin sphere radius) values utilized for La, Al, O and Cr atoms are 2.26, 1.51, 1.51 and 2.4 (a.u), respectively. The value of  $G_{max}=14$  is used for atomic radii conversion. The  $\text{LaAlO}_3$  possess cubic structure having space group of  $\text{Pm-3m}$  (221). The atoms of La are centered at (0.5, 0.5, 0.5), the Al are positioned at (0, 0, 0) whereas the three oxygen are situated at (0, 0.5, 0), (0, 0, 0.5) and (0.5, 0, 0) in crystal unit cell of  $\text{LaAlO}_3$ . When Cr is replaced at aluminum site in  $\text{LaAlO}_3$ , the atom is located at (0, 0, 0) in unit cell. The atomic radius is 2.50, 1.84, 2.00 and 1.52 (Å) for La, Al, Cr and O, respectively. The computed lattice parameters values for this compound are 3.79 Å. The electronic configuration of elements is  $[\text{Ne}]3s^23p^1$  for Al,  $[\text{Xe}]5d^16s^2$  for La,  $[\text{Ar}]3d^54s^1$  for Cr and  $[\text{He}]2p^42s^2$  for O.

## 3. Results and discussions

### 3.1. Electronic properties

The electronic behavior of Cr doped  $\text{LaAlO}_3$  based on BS, TDOS as well as PDOS are calculated with different concentrations of Cr doping as represented in Figs. 1-4. These properties are examined for  $\text{LaCr}_x\text{Al}_{1-x}\text{O}_3$  ( $x=0.125, 0.25, 0.50, \text{ and } 0.75$ ) and are computed in first Brillion-zone. The distance between VB maxima and CB minima gives value of  $E_g$ . It was examined that when we change doping concentration in  $\text{LaAlO}_3$ , the  $E_g$  varies improperly. The nature of  $E_g$  was determined as direct and indirect (see Fig. 1(a)) for  $\text{LaCr}_{0.125}\text{Al}_{0.875}\text{O}_3$  in spin up ( $\uparrow$ ) and spin down ( $\downarrow$ ) channel, respectively. When  $\text{LaAlO}_3$  was doped with 0.25 and 0.50 concentration of Cr, the  $E_g$  was calculated as indirect in both spin regions. Furthermore, the  $E_g$  value for  $\text{LaCr}_{0.25}\text{Al}_{0.75}\text{O}_3$  was observed as 0.22 and 0.05 eV (see Fig. 1(b)) in spin down ( $\downarrow$ ) and spin up ( $\uparrow$ ) channels, respectively. For  $\text{LaCr}_{0.50}\text{Al}_{0.50}\text{O}_3$ , the value of  $E_g$  (see Fig. 1(c)) in spin up ( $\uparrow$ ) and down ( $\downarrow$ ) region

was 0.34 and 2.65 eV. Moreover, behavior of  $E_g$  was computed as direct in spin up ( $\uparrow$ ) and indirect in spin down ( $\downarrow$ ) channel for  $\text{LaCr}_{0.75}\text{Al}_{0.25}\text{O}_3$  (see Fig. 1(d)).

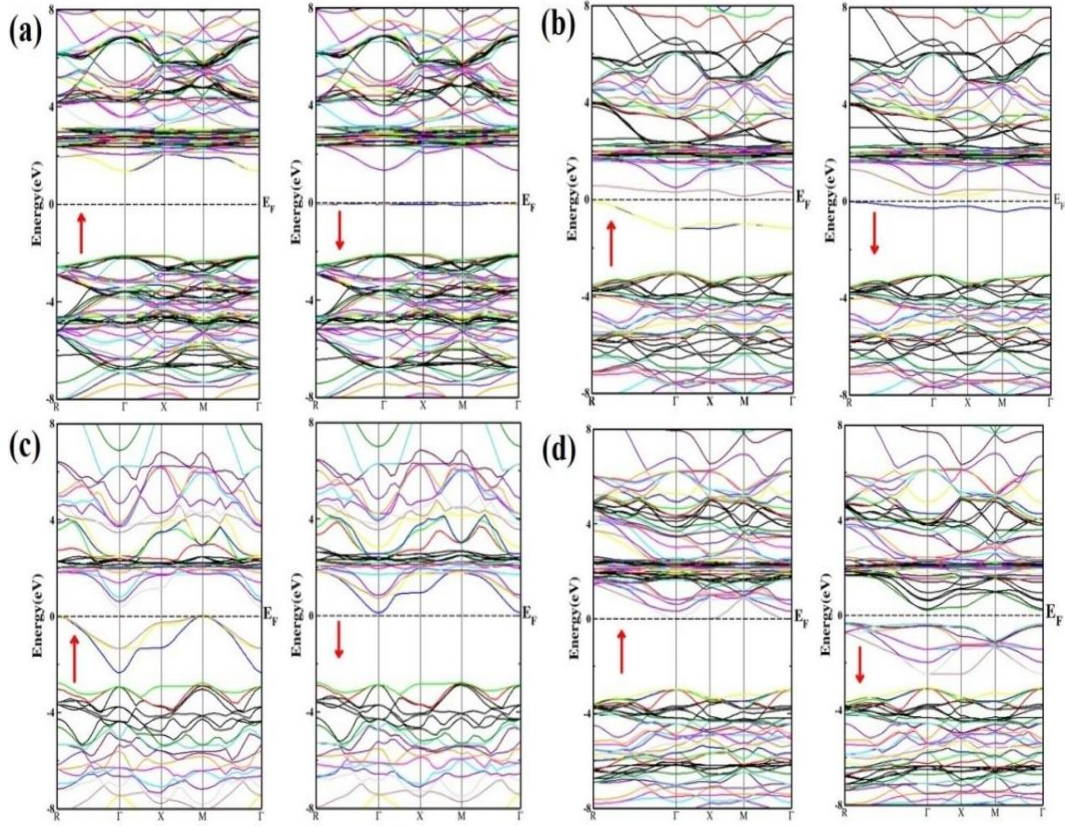


Fig. 1. BS of Cr doped  $\text{LaAlO}_3$  (a)  $\text{LaCr}_{0.125}\text{Al}_{0.875}\text{O}_3$  (b)  $\text{LaCr}_{0.25}\text{Al}_{0.75}\text{O}_3$  (c)  $\text{LaCr}_{0.50}\text{Al}_{0.50}\text{O}_3$  (d)  $\text{LaCr}_{0.75}\text{Al}_{0.25}\text{O}_3$ .

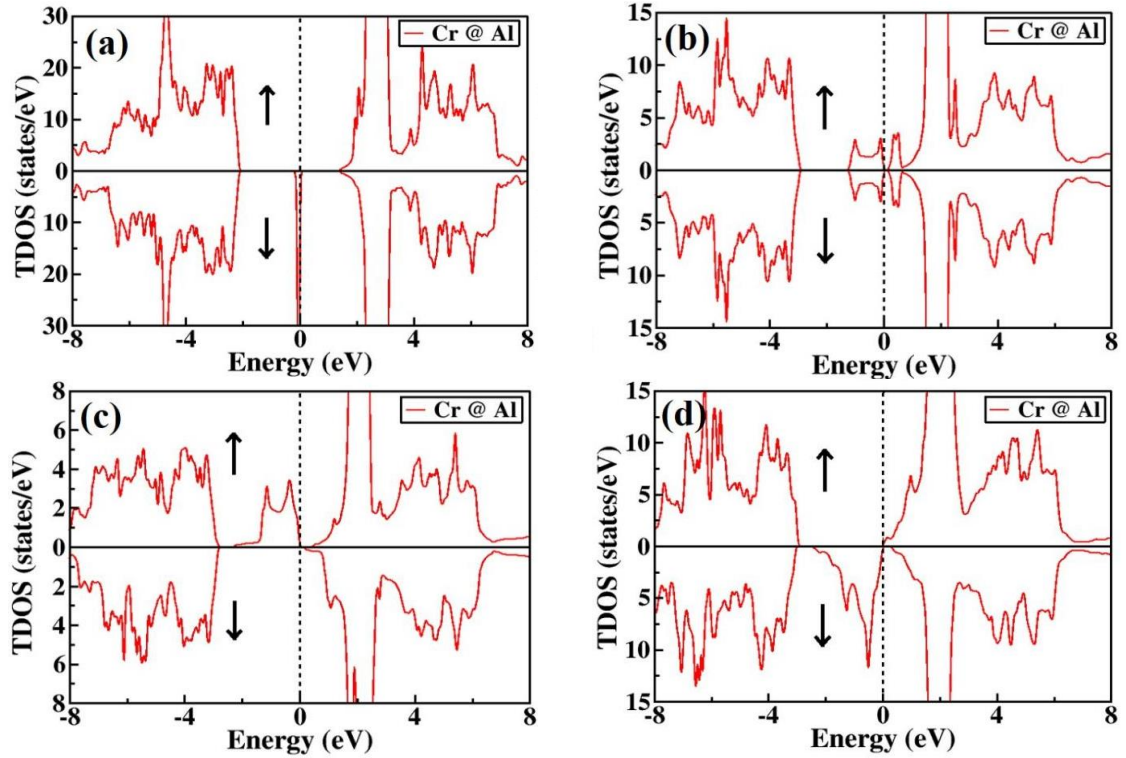


Fig. 2. TDOS of Cr doped  $\text{LaAlO}_3$  (a)  $\text{LaCr}_{0.125}\text{Al}_{0.875}\text{O}_3$  (b)  $\text{LaCr}_{0.25}\text{Al}_{0.75}\text{O}_3$  (c)  $\text{LaCr}_{0.50}\text{Al}_{0.50}\text{O}_3$  (d)  $\text{LaCr}_{0.75}\text{Al}_{0.25}\text{O}_3$ .

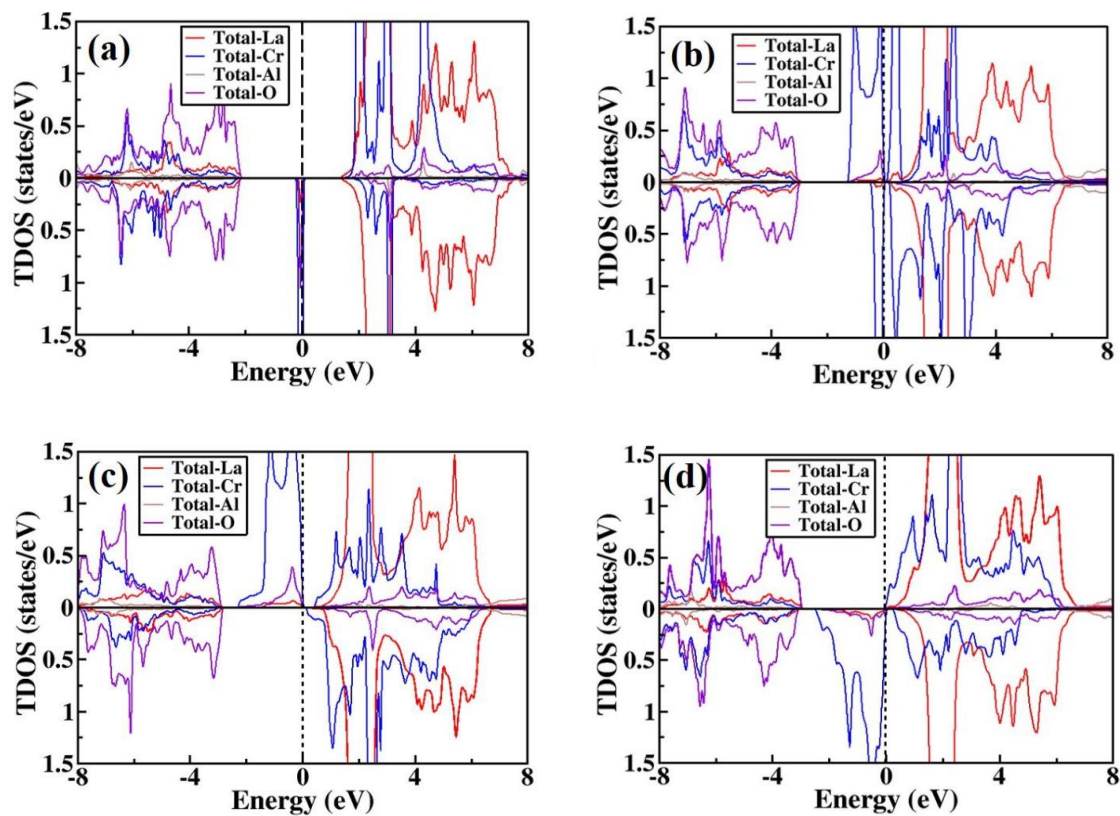


Fig. 3. Atomic TDOS of Cr doped  $\text{LaAlO}_3$  (a)  $\text{LaCr}_{0.125}\text{Al}_{0.875}\text{O}_3$  (b)  $\text{LaCr}_{0.25}\text{Al}_{0.75}\text{O}_3$  (c)  $\text{LaCr}_{0.50}\text{Al}_{0.50}\text{O}_3$  (d)  $\text{LaCr}_{0.75}\text{Al}_{0.25}\text{O}_3$ .

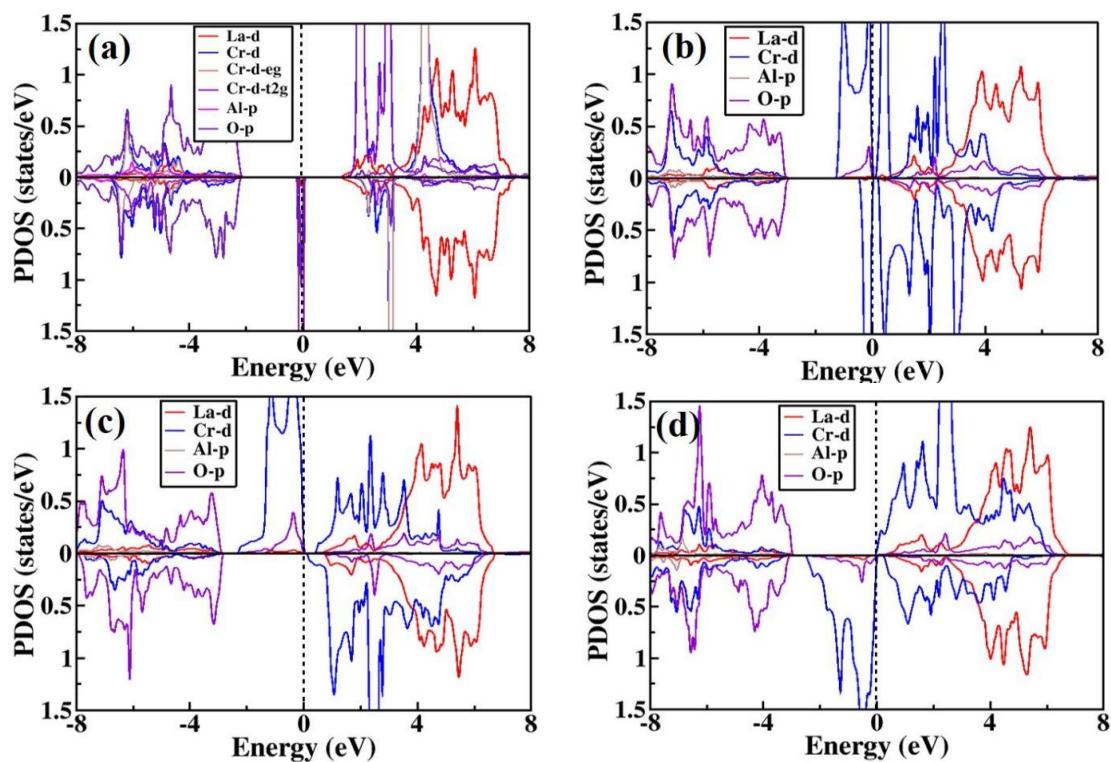


Fig. 4. PDOS of Cr doped  $\text{LaAlO}_3$  (a)  $\text{LaCr}_{0.125}\text{Al}_{0.875}\text{O}_3$  (b)  $\text{LaCr}_{0.25}\text{Al}_{0.75}\text{O}_3$  (c)  $\text{LaCr}_{0.50}\text{Al}_{0.50}\text{O}_3$  (d)  $\text{LaCr}_{0.75}\text{Al}_{0.25}\text{O}_3$ .

All computations of BS showed semiconductor behavior of compound under study. Moreover, we have computed electronic properties of LaAlO<sub>3</sub> in our previous research and found a band gap of 3.46 eV in its pure form [28].

The PDOS and TDOS for LaAlO<sub>3</sub> are computed at various concentrations of Cr (see Figs. 2-4). It can be seen in Fig. 4(a), for LaCr<sub>0.125</sub>Al<sub>0.875</sub>O<sub>3</sub>, the contribution of La-5*d* and Cr-3*d* is maximum in CB, whereas O-2*p* states have shown highest participation in VB in spin up (↑) and down (↓) channel. According to pseudo potential theory, the bond length decreases with the elevation in hybridization strength, and both these parameters plays significant role in electronic BS formation [29]. Hybridization strength between 2*p*(O) and 5*d*(La) is maximum at all concentrations of Cr in LaAlO<sub>3</sub>. When LaAlO<sub>3</sub> is doped with Cr at (x= 0.25 and 0.50), the Cr-3*d* and La-5*d* states coincide with Fermi level in CB whereas the involvement of O-2*p* is maximum as shown in Fig. 4(b & c). For LaCr<sub>0.75</sub>Al<sub>0.25</sub>O<sub>3</sub> compound, the influence of Cr, La and O states have dominating effect in conduction and VB for spin down (↓) and spin up (↑) channel, respectively.

### 3.2. Optical properties

The optical features of Cr doped LaAlO<sub>3</sub> can be observed in terms of conduction, absorption, dispersion, reflection, and polarization. The absorption and dispersion of electromagnetic radiation are observed by dielectric function which is schematically shown in Fig. 5(a & b). The dielectric constant and BS are directly related with each other. Moreover, the atoms interactions with incident photons are computed by frequency dependent dielectric constant. It contains real and imaginary part and can be expressed by the following relation [30]:

$$\varepsilon(\omega) = \varepsilon_1(\omega) + i\varepsilon_2 \quad (2)$$

The  $\varepsilon_1(\omega)$  displays the polarization of light while the  $i\varepsilon_2(\omega)$  is directly linked to absorption of incident light and electronic BS. Different optical properties such as  $\sigma(\omega)$ ,  $k(\omega)$ ,  $n(\omega)$ ,  $\alpha(\omega)$ , and  $R(\omega)$  are examined from imaginary part  $\varepsilon_2(\omega)$  of dielectric function. The  $\varepsilon_2(\omega)$  can be analyzed by the computations of BS using following relation:

$$\varepsilon_2(\omega) = \frac{e^2 \hbar}{\pi m^2 \omega^2} \sum_{vc} \int |n, n'(k, q)|^2 \delta[\omega_{n,n}(k) - \omega] d^3k \quad (3)$$

The  $\varepsilon_1(\omega)$  can be examined from the  $\varepsilon_2(\omega)$  with the help of Kramers-Kronig relationship [31]:

$$\varepsilon_1(\omega) = 1 + \frac{2}{\pi} p \int_0^\theta \frac{\omega' \varepsilon_2(\omega')}{\omega'^2 - \omega^2} d\omega' \quad (4)$$

The extreme values of  $\varepsilon_1(\omega)$  appear at 4.7, 4.61, 4.6 and 5.06 eV for LaCr<sub>x</sub>Al<sub>1-x</sub>O<sub>3</sub> at x= 0.75, 0.50, 0.25, 0.125, respectively (see Fig. 5 (a)). However, the highest value of  $\varepsilon_1(\omega)$  for pure LaAlO<sub>3</sub> is 5.26 eV [28]. After reaching at highest point, the values of  $\varepsilon_1(\omega)$  have shown fluctuations in high energy region because of variable transition rates. The imaginary part displays material ability to absorb light. The computed values of  $\varepsilon_2(\omega)$  are represented in Fig. 5(b) and maximum values of LaCr<sub>x</sub>Al<sub>1-x</sub>O<sub>3</sub> at (x=0.125, 0.25 0.50, 0.75) occurs at 7.58, 7.83, 7.83 and 8.31, respectively.

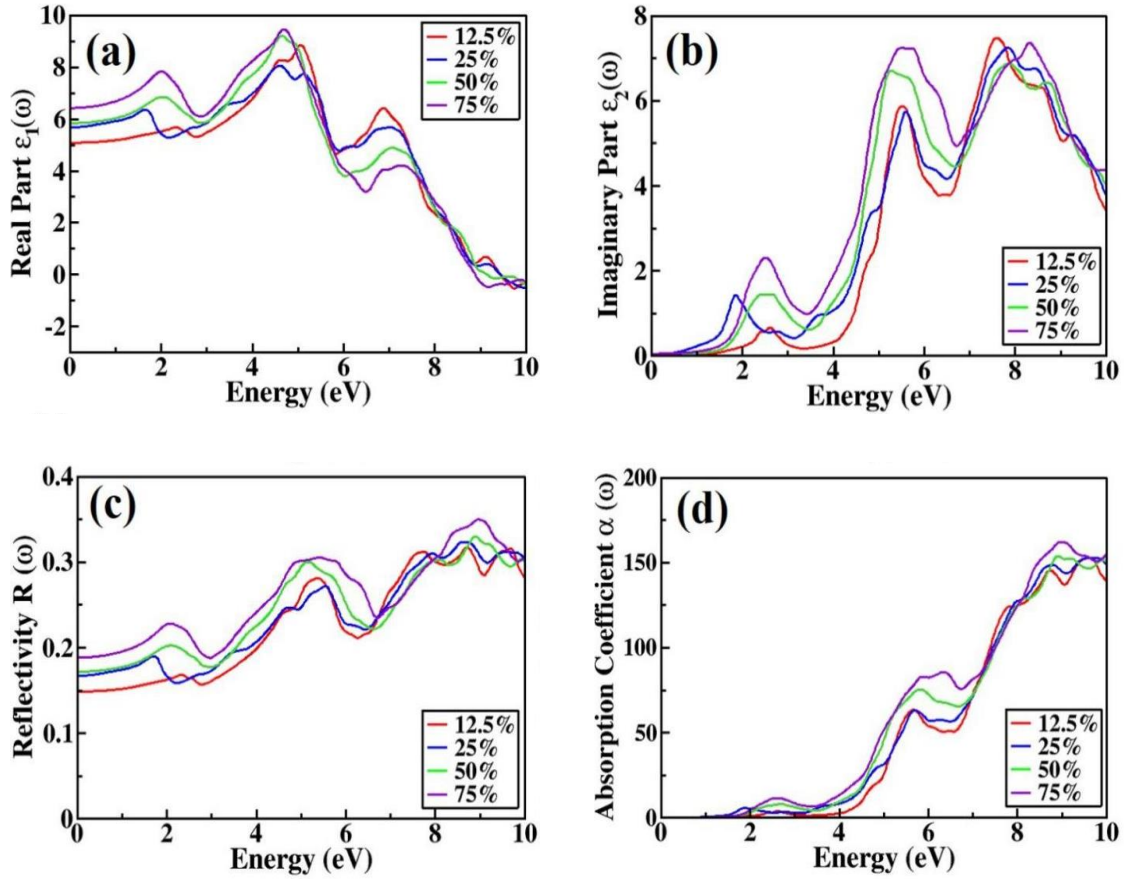


Fig. 5. (a)  $\varepsilon_1(\omega)$  (b)  $\varepsilon_2(\omega)$  (c)  $R(\omega)$  (d)  $\alpha(\omega)$  of Cr doped  $\text{LaAlO}_3$

The reflectivity is one of the most significant phenomena which described the features of compound to the falling light. The  $\varepsilon_1(\omega)$  values of dielectric function and  $R(\omega)$  displays the similar behavior. When the photon energy elevates, the reflectivity also elevates. The highest value of reflectivity (see Fig. 5(c)) occurs at 8.73, 8.63, 8.88 and 9 eV for  $\text{LaCr}_x\text{Al}_{1-x}\text{O}_3$  whereas ( $x = 0.125, 0.25, 0.50, 0.75$ ), respectively. The peaks appeared due to the inter-band transitions among valence and CB. The  $R(\omega)$  can be computed by using formulation:

$$R(\omega) = \frac{[n(\omega) - 1]^2 + k^2(\omega)}{[n(\omega) + 1]^2 + k^2(\omega)} \quad (5)$$

The  $k(\omega)$  and  $\alpha(\omega)$  are linked with one another through  $\alpha = 4\pi k/\lambda$ . The absorption of incident light lies in UV region (see Fig. 5(d)) which originates from 4 to 10 eV. The maximum absorption appears at 9.66, 9.77, 9.90 and 8.98 eV for 0.125, 0.25, 0.50 and 0.75 doping of Cr in Lanthanum Aluminate. Thus, the absorption of ultraviolet frequency is highest in this energy region which describes that this material is active in given energy range. The extinction coefficient of Cr doped  $\text{LaAlO}_3$  is computed, and the respective results are shown in Fig. 6(a). No changes are observed in  $k(\omega)$  values at 0 eV but changes with increments in amount of incident light. The maximum peak occurs at 1.66 for  $\text{LaAlO}_3$  without doping which is reported in our previous calculations [28]. The  $n(\omega)$  explains the propagation of light inside the compound, and it can be explained by the expression:

$$n(\omega) = \left( \frac{[\varepsilon_1^2(\omega) + \varepsilon_2^2(\omega)]^{\frac{1}{2}} + \varepsilon_1(\omega)}{2} \right)^{\frac{1}{2}} \quad (6)$$

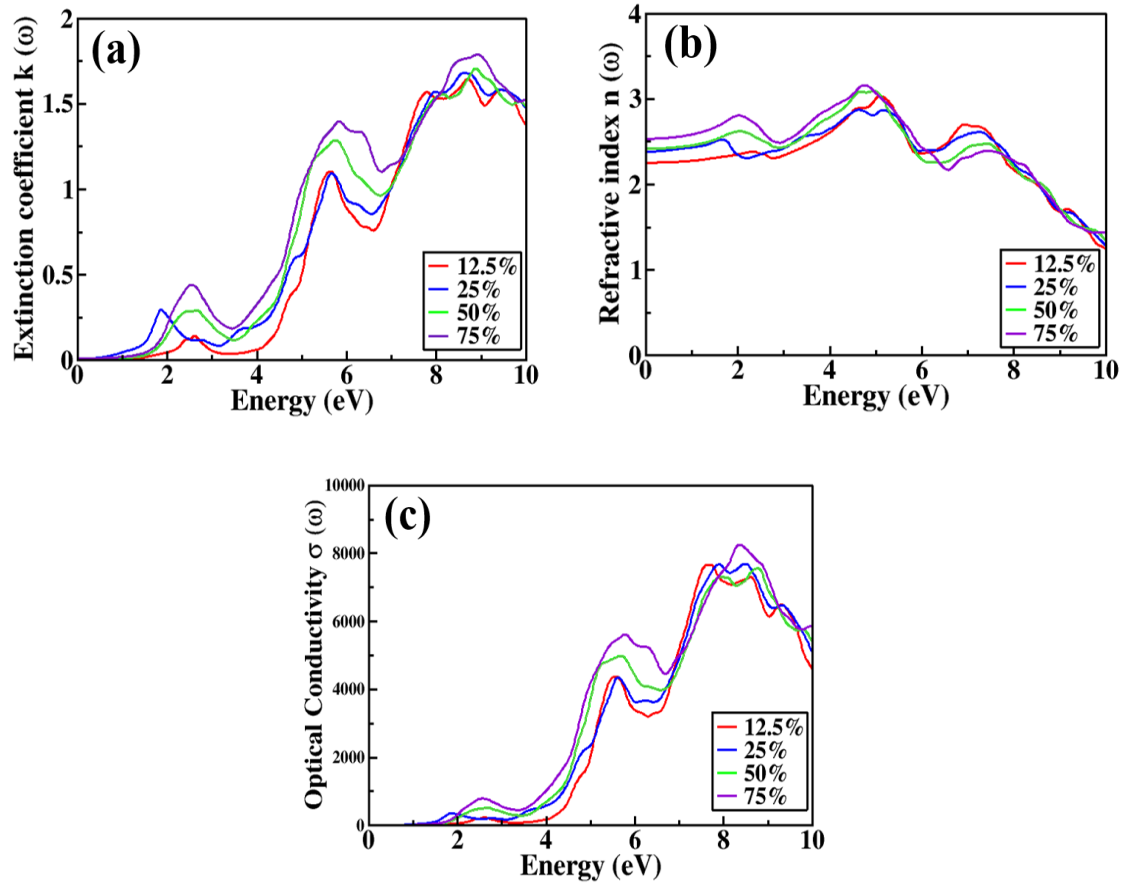


Fig. 6. (a)  $k(\omega)$  (b)  $n(\omega)$  (c)  $\sigma(\omega)$  of Cr doped  $\text{LaAlO}_3$

The  $\varepsilon_1(\omega)$ ,  $\varepsilon_2(\omega)$  and  $n(\omega)$  displays almost similar behavior, and these functions are related with each other through  $\varepsilon_1(\omega) = n^2 - k^2$  and  $\varepsilon_2(\omega) = 2nk$ . The values of  $n(\omega)$  are maximum at 5.089, 4.638, 4.981 and 4.76 for  $\text{LaCr}_x\text{Al}_{1-x}\text{O}_3$  ( $x = 0.125, 0.25, 0.50, 0.75$ ), respectively which is shown in Fig. 6(b). The bond breaking in the compound appears in relation to the electromagnetic radiations and it gives information about  $\sigma(\omega)$ . The  $\sigma(\omega)$  of Cr doped  $\text{LaAlO}_3$  is represented in Fig. 6(c). It can be seen that maximum values of  $\sigma(\omega)$  for Cr doping of 0.125, 0.25, 0.50 and 0.75 at 7.67, 8.49, 8.78 and 8.33, respectively.

### 3.3. Magnetic properties

The total, interstitial and individual magnetic moments are calculated by PBE-GGA [32]. To study the probable magnetism origin and effect of various spins, the results of different Cr concentration doping in  $\text{LaAlO}_3$  are summarized in Table 1. The effective magnetic moments of  $\text{LaCr}_x\text{Al}_{1-x}\text{O}_3$  at 0.125, 0.25, 0.50 and 0.75 is 3.00014, 3.00029, 3.00025 and 3.10847  $\mu_B$  respectively. It can be observed that highest magnetization occurs at  $x = 0.50$ . The magnetic properties of Cr doped Lanthanum aluminate depends upon direct exchange interaction. The direction of spin alignment can be indicated by sign of magnetic moments of various atoms. A negative magnetic moment of different atoms exposes anti ferromagnetic or ferromagnetic interaction whereas the positive sign value shows the spin alignment in the same direction [33]. The values of magnetic moment of Cr, Al, La and O atoms has opposite signs at all doping concentrations, which disclosed that all the atoms interact in ferromagnetic order. It is well reported from the magnetic outcomes of  $\text{LaCr}_x\text{Al}_{1-x}\text{O}_3$  that the compound is ferromagnetic in nature.

Table 1. Calculated  $M_{int}$ ,  $M_{La}$ ,  $M_{Cr}$ ,  $M_{Al}$ ,  $M_O$  and  $M_{Tot}$  in units of  $\mu_B$  for Cr doped  $LaAlO_3$  compound.

	$M_{int}$	$M_{La}$	$M_{Cr}$	$M_{Al}$	$M_O$	$M_{Tot}$
<b>0.125</b>	0.44869	0.01103	2.32365	0.00121	0.0228	3.00014
<b>0.25</b>	0.13868	0.00462	0.79543	-0.00081	0.07577	3.00029
<b>0.50</b>	0.49281	0.040333	2.26073	-0.00108	0.08357	3.00025
<b>0.75</b>	0.29688	-0.05787	2.67061	0.00236	0.18506	3.10847

#### 4. Conclusions

In this work, the magnetic, optical, and electronic properties of Cr doped Lanthanum aluminate are computed by FP-LAPW method. It is observed that Cr doped LAO is semiconductor in both spin channels. Inter-band transition depends on the doping of Cr element. The DOS plots have shown major involvement of Cr-3d, La-5d and O-2p. Meanwhile, various optical parameters such as  $R(\omega)$ ,  $\alpha(\omega)$ ,  $n(\omega)$ ,  $k(\omega)$  and  $a(\omega)$  are examined. Moreover, the computations of magnetic properties confirmed the ferromagnetic nature of  $LaCr_xAl_{1-x}O_3$ . All the results of Cr doped  $LaAlO_3$  indicates the suitability of this compound for potential uses in optoelectronic and spintronics devices.

#### Acknowledgements

The authors extend their appreciation to the Research Center for Advanced Materials Science (RCAMS), King Khalid University, Saudi Arabia, for funding this work under grant number KKU/RCAMS/G011-21. The authors also express their gratitude to Princess Nourah bint Abdulrahman University Researchers Supporting Project number PNURSP2022R81, Princess Nourah bint Abdulrahman University, Riyadh, Saudi Arabia.

#### References

- [1] L. S.Kouchaksaraie, International Journal of Mathematical, Computational, Physical, Electrical and Computer Engineering, 5(11), 1680-1683 (2011).
- [2] C.Azahaf, H.Zaari, A.Abbassi, H.Ez-Zahraouy, A. Ben-youssef, Optical and Quantum Electronics, 47(8), 2889-2897(2015); <https://doi.org/10.1007/s11082-015-0178-2>
- [3]M.K.Butt, M. Yaseen, I.A.Bhatti, J.Iqbal, A.Murtaza, M.Iqbal, M.mana AL-Anazy, M.H.Alhossainy, A.Laref, Journal of Materials Research and Technology, 9(6),16488-16496 (2020); <https://doi.org/10.1016/j.jmrt.2020.11.055>
- [4]M.K.Butt, M. Yaseen, J.Iqbal, A.S.Altowyan, A.Murtaza, M.Iqbal, A.Laref, Journal of Physics and Chemistry of Solids, 154,110084(2021); <https://doi.org/10.1016/j.jpcs.2021.110084>
- [5] R. B.Behram, M. A.Iqbal,S. M. Alay-e-Abbas, M.Sajjad, M.Yaseen, M. I.Arshad, G. Murtaza,Materials Science in Semiconductor Processing, 41, 297-303(2016); <https://doi.org/10.1016/j.mssp.2015.09.010>
- [6] S. A.Dar,V.Srivastava, U. K.Sakalle, V.Parey, G. Pagare, Materials Research Express, 4(10), 106104(2017); <https://doi.org/10.1088/2053-1591/aa90af>
- [7] S. A.Khandy,I. Islam, D.C.Gupta, A.Laref, Journal of molecular modeling, 24(6), 131 (2018); <https://doi.org/10.1007/s00894-018-3666-z>
- [8] Z. Y.Mao, Y. C.Zhu, Q. N.Fei, D. J.Wang, Journal of luminescence, 131(5), 1048- 1051 (2011); <https://doi.org/10.1016/j.jlumin.2011.01.020>
- [9]S.Saleem, S.A.Aldaghfag, M. Yaseen, M.K.Butt, M.Zahid, A.Murtaza, A.Laref, The European Physical Journal Plus, 137(1), 1-9(2022); <https://doi.org/10.1140/epjp/s13360-022-02352-z>

- [10] J. J. Ge, M. Yang, X. B. Xue, B. You, L. Sun, W. Zhang, J. Du, *physica status solidi c*, 9(1), 97-100(2012); <https://doi.org/10.1002/pssc.201084186>
- [11] Z. Han, X. Li, J. Ye, L. Kang, Y. Chen, J. Li, Z. Lin, *Journal of the American Ceramic Society*, 98(8), 2336-2339(2015); <https://doi.org/10.1111/jace.13706>
- [12] A. Sohail, S. A. Aldaghfag, M. K. Butt, M. Zahid, M. Yaseen, J. Iqbal, Misbah, M. Ishfaq, A. Dahshan, *Journal of Ovonic Research*, 17(5), 461-469 (2021).
- [13] H. Shafique, S. A. Aldaghfag, M. Kashif, M. Zahid, M. Yaseen, J. Iqbal, Misbah, R. Neffati, *Chalcogenide Letters*, 18(10), 589-599 (2021).
- [14] H. Ambreen, S. A. Aldaghfag, M. Yaseen, J. Iqbal, M. Zahid, A. Dahshan, H. H. Hegazy, *Physica Scripta*, 97(6), 065807 (2022); <https://doi.org/10.1088/1402-4896/ac6910>
- [15] M. Mączka, A. Bednarkiewicz, E. Mendoza-Mendoza, A. F. Fuentes, L. Kępiński, *Journal of Solid State Chemistry*, 194, 264-269(2012); <https://doi.org/10.1016/j.jssc.2012.05.035>
- [16] S. A. Aldaghfag, M. Yaseen, H. Ambreen, M. K. Butt, A. Dahshan, *Chalcogenide Letters*, 18(7), 357-365 (2021).
- [17] H. Wang, L. Zhang, C. Hu, X. Wang, L. Lyu, G. Sheng, *Chemical Engineering Journal*, 332, 572-581(2018); <https://doi.org/10.1016/j.cej.2017.09.058>
- [18] M. Rizwan, S. Gul, T. Mahmood, M. Shakil, A. Majid, M. Rafique, C. B. Cao, *Canadian Journal of Physics*, 99(1), 38-43(2021); <https://doi.org/10.1139/cjp-2019-0558>
- [19] M. Mączka, A. Bednarkiewicz, E. Mendoza-Mendoza, A. F. Fuentes, L. Kępiński, *Journal of Solid State Chemistry*, 194, 264-269(2012); <https://doi.org/10.1016/j.jssc.2012.05.035>
- [20] A. Dhahri, K. Horchani-Naifer, A. Benedetti, F. Enrichi, M. Ferid, P. Riello, *Optical Materials*, 35(6), 1184-1188(2013); <https://doi.org/10.1016/j.optmat.2013.01.013>
- [21] Y. Katayama, H. Kobayashi, S. Tanabe, *Applied Physics Express*, 8(1), 012102(2014); <https://doi.org/10.7567/APEX.8.012102>
- [22] M. R. Benam, N. Abdoshahi, M. M. Sarmazdeh, *Computational materials science*, 84, 360-364(2014); <https://doi.org/10.1016/j.commatsci.2013.12.034>
- [23] A. Boudali, B. Amrani, A. Abada, K. Amara, *Computational materials science*, 45(4), 1068-1072(2009); <https://doi.org/10.1016/j.commatsci.2009.01.011>
- [24] J. P. Perdew, K. Burke, M. Ernzerhof, *Physical review letters*, 77(18), 3865(1996); <https://doi.org/10.1103/PhysRevLett.77.3865>
- [25] Z. Ali, I. Khan, I. Ahmad, M. S. Khan, S. J. Asadabadi, *Materials Chemistry and Physics*, 162, 308-315(2015); <https://doi.org/10.1016/j.matchemphys.2015.05.072>
- [26] G. Murtaza, N. Yousaf, A. Laref, M. Yaseen, *Zeitschrift für Naturforschung A*, 73(4), 285-293(2018); <https://doi.org/10.1515/zna-2017-0388>
- [27] S. Naeem, G. Murtaza, R. Khenata, M. N. Khalid, *Physica B: Condensed Matter*, 414, 91-96 (2013); <https://doi.org/10.1016/j.physb.2013.01.009>
- [28] M. Yaseen, A. Ashfaq, A. Akhtar, R. Asghar, H. Ambreen, M. K. Butt, A. Murtaza, *Materials Research Express*, 7(1), 015907(2020); <https://doi.org/10.1088/2053-1591/ab6110>
- [29] M. Imada, A. Fujimori, Y. Tokura, *Reviews of modern physics*, 70(4), 1039(1998); <https://doi.org/10.1103/RevModPhys.70.1039>
- [30] B. Amin, I. Ahmad, M. Maqbool, S. Goumri-Said, R. Ahmad, *Journal of Applied Physics*, 109(2), 023109(2011); <https://doi.org/10.1063/1.3531996>
- [31] M. Yaseen, H. Ambreen, A. Sufyan, M. K. Butt, S. Ur-Rehman, J. Iqbal, S. M. Ramay, *Ferroelectrics*, 557(1), 112-122(2020).
- [32] M. Yaseen, H. Ambreen, J. Iqbal, A. Shahzad, R. Zahid, N. A. Kattan, A. Mahmood, *Philosophical Magazine*, 100(24), 3125-3140(2020); <https://doi.org/10.1080/14786435.2020.1812748>
- [33] Q. Mehmood, M. Hassan, M. Yaseen, A. Laref, *Chemical Physics Letters*, 729, 11-16 (2019); <https://doi.org/10.1016/j.cplett.2019.05.011>